Genetic correction and analysis of induced pluripotent stem cells from a patient with gyrate atrophy

Sara E. Howden[a,b,c], Athurva Gore[d], Zhe Li[d], Ho-Lim Fung[d], Benjamin S. Nisler[e], Jeff Nie[a], Goukai Chen[a,b,c], Brian E. McIntosh[a,b,c], Daniel R. Gulbranson[a,b,c], Nicole R. Diol[a,b,c], Seth M. Taapken[e], David T. Vereide[a,b,c], Karen Dyer Montgomery[e], Kun Zhang[d], David M. Gamm[f], and James A. Thomson[a,b,c,g,1]

[a]Morgridge Institute for Research, Madison, WI 53715; [b]Department of Cell and Regenerative Biology, University of Wisconsin School of Medicine and Public Health, Madison, WI 53707-7365; [c]Genome Center of Wisconsin, University of Wisconsin, Madison, WI 53706; [d]Department of Bioengineering, University of California at San Diego, La Jolla, CA 92093; [e]Wicell Research Institute, Madison, WI 53707; [f]Department of Ophthalmology and Visual Sciences, Waisman Center Stem Cell Research Program, Eye Research Institute, University of Wisconsin, Madison, WI 53705; and [g]Department of Molecular, Cellular, and Developmental Biology, University of California, Santa Barbara, CA 93106

Contributed by James A. Thomson, March 1, 2011 (sent for review January 21, 2011)

Gene-corrected patient-specific induced pluripotent stem (iPS) cells offer a unique approach to gene therapy. Here, we begin to assess whether the mutational load acquired during gene correction of iPS cells is compatible with use in the treatment of genetic causes of retinal degenerative disease. We isolated iPS cells free of transgene sequences from a patient with gyrate atrophy caused by a point mutation in the gene encoding ornithine-δ-aminotransferase (*OAT*) and used homologous recombination to correct the genetic defect. Cytogenetic analysis, array comparative genomic hybridization (aCGH), and exome sequencing were performed to assess the genomic integrity of an iPS cell line after three sequential clonal events: initial reprogramming, gene targeting, and subsequent removal of a selection cassette. No abnormalities were detected after standard G-band metaphase analysis. However, aCGH and exome sequencing identified two deletions, one amplification, and nine mutations in protein coding regions in the initial iPS cell clone. Except for the targeted correction of the single nucleotide in the *OAT* locus and a single synonymous base-pair change, no additional mutations or copy number variation were identified in iPS cells after the two subsequent clonal events. These findings confirm that iPS cells themselves may carry a significant mutational load at initial isolation, but that the clonal events and prolonged cultured required for correction of a genetic defect can be accomplished without a substantial increase in mutational burden.

Autologous therapies based on induced pluripotent stem (iPS) cells (1–3) have the potential to treat a wide range of acquired and inherited diseases, but the extensive culture period required could introduce a mutational burden incompatible with specific clinical applications. For example, diabetes is a disease that continues to have a serious impact on quality and length of life despite its clinical management with insulin and is an attractive target for iPS cell-based transplantation therapies. However, pancreatic cancer is generally fatal within a few months of diagnosis. Thus, it will be essential to determine the accumulated mutational load of cells before transplantation and to determine whether these mutations may lead to a significantly increased risk of oncogenesis. A recent study revealed that a significant number of point mutations are generally present in iPS cell clones relative to the average sequence of the parental somatic cells (4). Exome sequencing of 22 independent human iPS cell lines reprogrammed by using four different methods revealed a range of 1–14 point mutations in each of the lines analyzed, with a projected average of six protein-coding mutations per genome.

Because of the proliferative potential of iPS cells, homologous recombination can be used to correct specific genetic defects before transplantation. However, gene targeting typically requires prolonged culture, drug selection, and additional clonal genetic bottlenecks beyond initial iPS cell generation and may, therefore, be expected to introduce high mutational loads. Here, we assess the mutational load accumulated in iPS cells after three clonal events that led to the targeted correction of a single base-pair mutation in the *OAT* locus.

Homozygous mutations in the *OAT* locus result in Gyrate atrophy (GA) of the choroid and retina, a disease characterized by progressive loss of visual acuity and night vision with eventual loss of central vision typically occurring in the fourth to fifth decades of life (5). Although the exact pathophysiological mechanism of GA remains unknown, the retinal pigmented epithelium (RPE) is thought to be the initial site of degeneration (6). RPE dysfunction is also involved in macular degeneration, the leading cause of incurable blindness in developed countries, affecting >14 million people worldwide (7). Diseases involving the RPE are attractive targets for iPS cell-based therapies, because there are already protocols for deriving RPE from human iPS cells (8, 9) and the site can be easily monitored with noninvasive techniques. Furthermore, the physiological function of the RPE depends on fairly simple anatomical relationships so it is reasonable to expect that transplanted cells could sustain retinal function if the structural damage is not yet too severe. Indeed, a recent study has demonstrated protective effects of iPS-derived RPE after transplantation into RCS dystrophic rats (10), and the two most recent human embryonic stem (ES) cell clinical trials approved in the United States involves transplantation of RPE cells (11).

In this study, we used an episomal reprogramming method (12) to generate iPS cells free of transgene sequences from a GA patient homozygous for a deleterious mutation in the *OAT* gene. We then used homologous recombination with a BAC-based vector to correct the disease-causing mutation. Vector-free, correctly targeted iPS cell clones were identified by custom high-density array comparative genomic hybridization (aCGH) and confirmed by standard techniques. We also performed sequential aCGH and exome sequencing of the parental fibroblast line, the iPS cell line before targeting, the iPS cell line after gene targeting, and the iPS cell line after removal of the selection cassette to assess the accumulation of genomic changes during these procedures. We found that although there was a fairly substantial mutational load in the iPS cell line at the time of derivation before targeting, homologous recombination and cassette removal could be carried out with minimal additional changes. These results suggest that the accumulation of mutations may

Author contributions: S.E.H., K.Z., D.M.G., and J.A.T. designed research; S.E.H., A.G., Z.L., H.-L.F., B.S.N., J.N., G.C., B.E.M., D.R.G., N.R.D., S.M.T., and K.D.M. performed research; A.G., Z.L., H.-L.F., B.S.N., J.N., S.M.T., and K.D.M. contributed new reagents/analytic tools; S.E.H., A.G., Z.L., H.-L.F., B.S.N., J.N., S.M.T., D.T.V., K.D.M., and K.Z. analyzed data; and S.E.H. and J.A.T. wrote the paper.

The authors declare no conflict of interest.

Freely available online through the PNAS open access option.

[1]To whom correspondence should be addressed. E-mail: jthomson@morgridgeinstitute.org.

This article contains supporting information online at www.pnas.org/lookup/suppl/doi:10.1073/pnas.1103388108/-/DCSupplemental.

GENETICS

not limit the clinical utility of gene targeting approaches, but that extensive genetic characterization of the initial iPS cell clones will be critical.

Results

We obtained primary dermal fibroblasts from a GA patient from the Coriell Institute for Medical Research. This donor is homozygous for a C > T transition at nucleotide 677 (677C > T) in exon 7 of the *OAT* gene that converts alanine 226 (GCG) to valine (GTG). To generate patient-specific iPS cells free of transgene sequences, we used an episomal reprogramming strategy based on the transfection of *oriP*-containing plasmid vectors encoding seven reprogramming factors (OCT4, SOX2, NANOG, LIN28, c-Myc, KLF4, and SV40 large T-antigen) (12). These EBV-based episomal vectors are replicated in synchrony with the host cells and are relatively stable, but in the absence of selection, are nonetheless lost from dividing cells at a rate of ≈2–6% per cell generation (13, 14), allowing the vectors to persist long enough to induce reprogramming before being ultimately lost, resulting in iPS cells that are free of transgene sequences. After a single transfection, iPS cell clones were selected based on basic morphological criteria (e.g., compact colonies, high nucleus-to-cytoplasm ratios, and prominent nucleoli) and six clones were expanded for further analysis. Total DNA was extracted and PCR analysis was performed to examine whether episomal DNA used for reprogramming remained. In four iPS cell clones, episomal sequences were not detected (Fig. S1).

Two iPS cell lines (5 and 12) were selected for subsequent gene targeting experiments. We designed a gene targeting construct carrying a 37.4-kb fragment from a human BAC clone that encodes the entire *OAT* coding region. A puromycin resistance cassette flanked by loxP sites was inserted just downstream of the *OAT* coding region, resulting in two homologous arms ≈27.7 kb and 8.8 kb in size (Fig. 1). We successfully isolated and expanded 15 and 5 puromycin-resistant colonies after the electroporation of the linearized targeting vector into iPS cell clones 5 and 12, respectively. Genomic DNA was extracted from each clone, and PCR analysis was performed to test for the presence of vector backbone sequences because clones that had undergone the desired homologous recombination event should not contain these sequences (Fig. S2). To assess expression of wild-type (w/t) *OAT* mRNA, total RNA was extracted and RT-PCR was performed to amplify exon 7 of the *OAT* transcript, which was then sequenced. Exon 7 of the *OAT* gene was also amplified from the genomic DNA of each iPS cell clone and sequenced. After scoring each line for the presence or absence of vector backbone sequences and a w/t copy of the *OAT* gene and/or transcript (Table S1), we identified two potential gene-targeted iPS cell clones (5.12 and 12.4). These two clones also displayed an almost 1:1 ratio of mutant to w/t transcript as evidenced by sequencing analysis of the *OAT* RT-PCR products (Fig. 2*A*). Fluorescent in situ hybridization (FISH) analysis revealed only two signals corresponding to the endogenous *OAT* loci on chromosome 10q26 and failed to detect any additional random integration events in these clones (Fig. 2*B*). FISH analysis performed on an iPS cell clone in which backbone targeting vector sequences were detected by PCR revealed the two endogenous loci and a third signal corresponding to a random integration event (Fig. 2*C*). Although we confirmed a gene targeting event in 2 of 20 (10%) drug-resistant clones, we could not detect a w/t copy of the *OAT* gene or transcript or any vector backbone sequences in 10 (50%) clones. Therefore, we cannot exclude that these clones did undergo homologous recombination but with a crossing over event occurring between exon 7 and the puromycin cassette rather than upstream of exon 7 (Fig. 1).

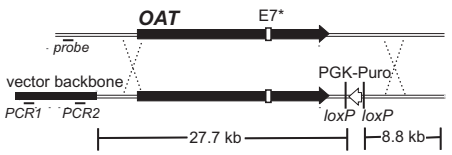

Fig. 1. Schematic diagram of the BAC-based gene targeting vector used in the study. A loxP-flanked selection cassette (PGK-Puro) was inserted ≈2 kb downstream of the *OAT* coding region by recombineering. The sizes of the homologous arms are shown. The point mutation in exon 7 (E7*), the regions amplified by PCR to identify random integrants, and the probe used in Southern blot experiments are also indicated.

We next wished to examine whether aCGH could also be used as a method to distinguish gene-targeted iPS cell clones from drug-resistant clones arising from random integration of the gene targeting vector. Genomic DNA from a gene-targeted iPS line (clone 12.4) and a random integrant (clone 5.15) confirmed by FISH were mixed with sex-mismatched reference DNA and then hybridized to a custom-designed array containing probes spanning our *OAT* gene targeting vector. No copy number variation (CNV) involving the *OAT* coding sequence could be detected for the gene-targeted line (clone 12.4) or its parental iPS cell line, whereas increased hybridization corresponding to the integrated puromycin cassette was observed as expected (Fig. 3*A*). Furthermore, CNV was not detected across the endogenous *OAT* locus, providing further evidence that homologous recombination of the gene targeting vector had occurred in iPS cell line 12.4 (Fig. 3*B*). In contrast, in the random integrant (5.15), we detected more than two copies of the *OAT* gene along with the puromycin cassette and all of the gene targeting vector backbone sequences (Fig. 3 *A* and *B*).

Our custom array was also designed to include probe sequences spanning the three episomal vectors used for reprogramming. We detected no vector sequences for the gene-targeted line (clone 12.4) and its parental iPS cell line (clone 12), but an ≈1,850-bp region of the reprogramming vectors corresponding to the 5′ end of *oriP* and C-terminal portion of the EBNA1 gene was detected in both the random integrant (clone 5.15) and its parental iPS cell line (clone 5) (Fig. 2*C*). PCR analysis using primers specific to this sequence confirmed its presence in iPS cell lines 5, 5.12, and 5.15 but not 12 or 12.4 (Fig. S3). These results indicate that, in addition to confirming homologous recombination, aCGH is useful in excluding any iPS cell clones with integrated vector sequences.

Although all clones had normal karyotypes after G-banding analysis, aCGH analysis revealed a number of subkaryotypic alterations in both the parental and gene-corrected iPS cells that were not detected after aCGH analysis of the original patient fibroblast line. These genomic alterations included two small deletions in the random integrant (clone 5.15) and its parental line (clone 5), and two separate small deletions and a single amplification in the gene-targeted line (clone 12.4) and its parental line (clone 12) (Table 1). No additional genomic aberrations were detected by aCGH in the gene-targeted iPS cell line (clone 12.4) compared with its parental iPS cell line (clone 12). Analysis of iPS cells derived from the same patient line but using lentiviral vectors also revealed several other amplifications and deletions, indicating that reprogramming with episomal vectors per se is unlikely to be the cause of large-scale genomic aberrations.

To remove the puromycin cassette, we transfected in vitro transcribed mRNA-encoding Cre recombinase into the gene-targeted iPS cell line (clone 12.4). Loss of the selection cassette was observed in 8/8 independent colonies as evidenced by sensitivity to puromycin in the culture medium and by PCR analysis of the extracted genomic DNA (Fig. S4*A*). One clone (12.4.2) was selected for further analysis. Southern blot confirmed the loss of the puromycin cassette and G-band analysis confirmed a normal karyotype (Fig. S4 *B* and *C*). Furthermore, when cells from this line were injected into immunocompromised mice, we

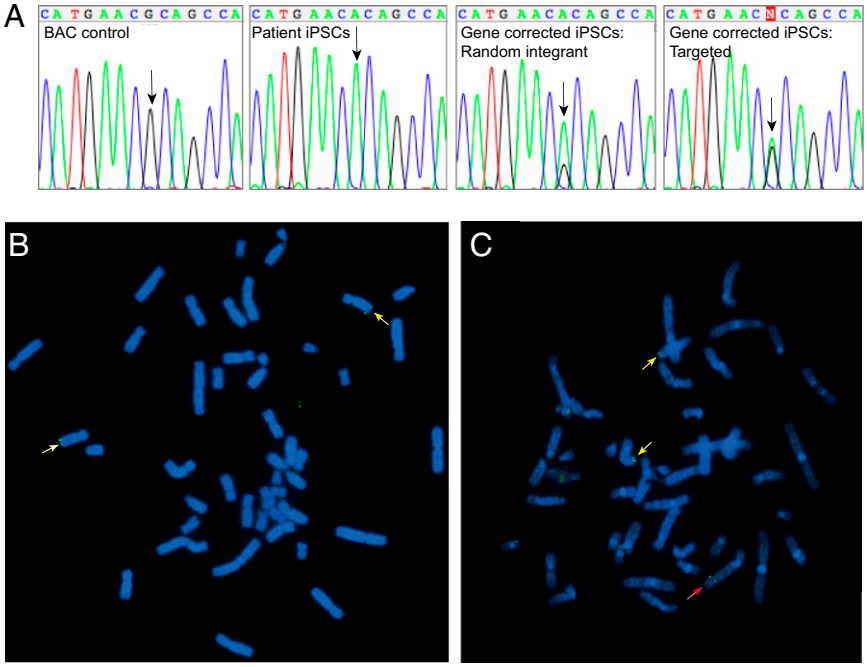

Fig. 2. Gene correction of patient iPS cells. (*A*) Chromatograms resulting from Sanger sequencing of *OAT* exon 7 PCR products amplified from the gene targeting vector or cDNA from an uncorrected iPS cell line and gene-corrected iPS cell lines arising from a random integration or gene targeting event. Arrows indicate the location of the point mutation in the patient line. The antisense strand is shown. FISH analysis of a gene-targeted iPS cell line (*B*) and a random integrant (*C*) using a fluorescently labeled probe specific to the *OAT* locus. Yellow arrows indicate endogenous signals on chromosome 10q; red arrow indicates a third signal caused by random integration of the gene-targeting construct.

observed teratomas comprising all three primary germ layers (Fig. S5). This line was also analyzed by aCGH, which also revealed loss of the puromycin cassette, lack of CNV at the *OAT* locus, absence of any reprogramming vector sequences, and lack of additional changes in genome integrity in comparison with its parental iPS cell lines (Fig. S6).

To investigate the accumulation of mutations through reprogramming, prolonged iPS cell culture, and the serial clonal events needed for gene targeting, we performed exome sequencing on the parental patient fibroblast cell line, an uncorrected iPS cell line (clone 12), the gene-targeted iPS cell line (clone 12.4), and the cassette-free iPS cell line (clone 12.4.2). We searched for novel mutations between each successive clonal line relative to its direct progenitor cell line sequence and discovered nine mutations in the original iPS cell clone (Table 2). Somewhat surprisingly, the genomes were remarkably stable through the subsequent clonal events. Exome sequencing successfully detected the correct 677T > C substitution introduced by homologous recombination in the gene-corrected iPS cell lines (clones 12.4 and 12.4.2). Although all nine original mutations were confirmed, no additional mutations were detected in the targeted iPS cell line (clone 12.4), and only one additional synonymous mutation was detected in the cassette-free iPS cell line (clone 12.4.2).

Discussion

A central challenge to the therapeutic use of either human iPS or ES cells is understanding what specific types and number of mutations and genomic aberrations are clinically acceptable for a given application, for such changes will always accumulate with continued cell division. Indeed, recent analyses of large sets of iPS cell lines identified a substantial number of cell lines carrying full and partial chromosomal aberrations that arose either from culture adaptation or from clonal selection of the parental cell line (15, 16). Although all of the iPS cell lines in this study had normal karyotypes by standard G-band analysis, aCGH and exome sequencing revealed at least three regions of CNV and nine mutations in the original iPS cell line before targeting. These findings are comparable to the results of other recent studies, suggesting that iPS cells themselves may carry a significant number of genomic aberrations and protein-coding mutations arising either in the donor, during somatic cell expansion, or during reprogramming itself (4). Importantly, we found that our current culture conditions can allow extensive expansion and genetic manipulations of human iPS without a dramatic increase in genomic instability and mutational burden. Clearly additional studies are required to better estimate the mutational load acquired during iPS cell culture, yet our results nonetheless allow an initial crude estimate of this load. The observation that only a single point mutation was acquired after gene correction and cassette removal is consistent with the expected load based on the average mutation rate in human somatic cells, while also being above the expected load based on average mutation rate in human germ-line cells (17).

Although BAC vectors have widely been used for the genetic modification of murine ES cells, only a single study had reported the use of BAC-based vectors for gene targeting in human pluripotent stem cells (18). Here, we demonstrate the use of a BAC-based homologous recombination strategy to successfully repair a single base-pair mutation in a patient-specific iPS cell line that is also free of reprogramming transgenes. We also found that transfection of mRNA-encoding Cre recombinase is a highly efficient method for removal of a loxP-flanked selection cassette in gene-corrected iPS cells. Although the residual 35-bp loxP site that remains in the genome of the cassette-free iPS cells is unlikely to have any detrimental effect, it would nonetheless be desirable to have the correction be entirely seamless. A seamless correction could be achieved by performing two sequential homologous recombinations, using both positive and negative selection, or by flanking the selection cassette with terminal repeats

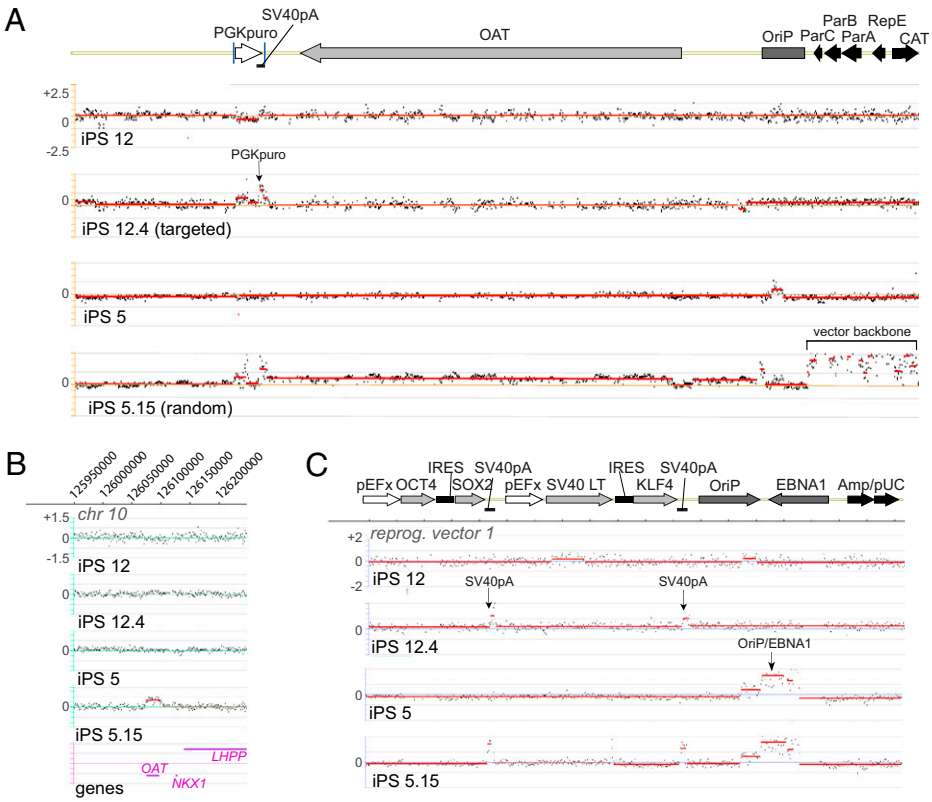

Fig. 3. High-density aCGH analysis of gene-corrected iPS cells. aCGH data for the *OAT* gene targeting vector (*A*), endogenous *OAT* locus (*B*), and one of the three reprogramming vectors (*C*) are shown for gene-corrected iPS cells resulting from a gene targeting (clone 12.4) or random integration (clone 5.15) event. Data for the two parental iPS cells (clones 12 and 5) are also shown.

from the piggyBac transposon, which can be seamlessly excised after transient expression of the piggyBac transposase (19).

In this study, we used an episomal approach to produce integration-free iPS cells, which has the advantage of requiring just a single transfection. Although there are now several other approaches to produce vector-free iPS cells, including seamless removal of piggyBac vectors (20), protein transduction (21), and RNA transfection (22), previous exome sequencing studies failed to find differences in mutational load between iPS cells derived by integration-free episomal or RNA methods, or between methods that included SV40 large T-antigen and those that did not (4). Although episomal sequences have the potential to integrate into the genome, as evidenced in this study, the detailed characterization required to assess genomic integrity of iPS cell clones could simultaneously be used to identify and exclude any iPS cell clones carrying integrated transgenes with no additional cost to the analysis. We demonstrate the feasibility of using customized aCGH for this purpose.

The mutational load observed in our iPS cell line is within the range of mutations detected in the recent exome sequencing study of 22 different iPS cell lines (4). Interestingly, analyses in that report revealed that a majority, but not all, of these mutations were present in subpopulations of the parental cell lines. Therefore, simply changing iPS cell generation methods or culture conditions cannot eliminate such mutations. Because iPS cell lines from different patients will also have unique sets of mutations, it will be extremely challenging to assign relative risks to different combinations of mutations. Clearly an ongoing di-

Table 1. Genomic aberrations identified in patient iPS cell lines by aCGH

iPS line	Chromsome	Region	Size	Type	Genes
12, 12.4	1p21.3	96856539–97322458	466 Kb	Del	1
	3p12.1	85211683–85484482	273 Kb	Del	2
	5q23.3	128528748–128683706	155 Kb	Amp	0
5, 5.15	10p11.22	32837303–33179113	341 Kb	Del	2
	13q31.3–32.1	93745041–93803505	58 Kb	Del	1
5.15	10q26.13	126073879–126101050	27 Kb	Amp	1 (*OAT*)
	20q11.21	29297062–30479976	1.2 Mb	Amp	>20
V*	1p21.3	97832565–97927692	95 Kb	Amp	1
	3q11.2	99239999–99546452	306 Kb	Amp	6
	6q25.1	151460582–151594818	134 Kb	Amp	2
	6q27	168184657–168243139	58 Kb	Del	2
	7p13	44222051–44300697	79 Kb	Del	1

*Patient iPS line generated with lentiviral reprogramming vectors.

Table 2. Mutations in protein coding regions identified via exome sequencing

iPS cell line	Mutation (chromosome, position, bases)	Gene	Codons	AA Sub.	SNP type	SIFT functional prediction	Gene mutated in cancer? (COSMIC)
12, 12.4, 12.4.2	15,40166820,G/A	PLA2G4D	GCC-GCt	A75A	Synonymous	N/A	No
	14,21172795,T/C	OR10G2	GAT-GgT	D15G	Nonsynonymous	Tolerated	No
	14,63713924,GG/AA	SYNE2	GAG-GAa	E2227E	Synonymous	N/A	Yes
			GAC-aAC	D2228N	Nonsynonymous	Damaging	
	18,18783610,AAA/GAC	RBBP8	AAA-gAc	K62E	Nonsynonymous	Tolerated	Yes
	19,58264996,C/A	ZNF160	ATG-ATt	M201I	Nonsynonymous	Tolerated	Yes
	13,42464175,C/G	EPSTI1	GGT-cGT	G43R	Nonsynonymous	Tolerated	No
	19,6263204,T/C	ACER1	ATA-ATg	I102M	Nonsynonymous	Tolerated	No
	19,826291,C/A	MED16	AGC-AtC	S575I	Nonsynonymous	Damaging	No
	17,44364015,G/A	SNF8	CGG-tGG	R210W	Nonsynonymous	Damaging	No
12.4, 12.4.2	10,126082451,G/A	OAT	GTG-GcG	V226A	Nonsynonymous	N/A (Corrected)	No
12.4.2	11,62157118,C/A	GANAB	CTG-CTt	L250L	Synonymous	N/A	Yes

N/A (not applicable) is listed for the three mutations that are synonymous or the gene-corrected base-pair change that was brought about by homologous recombination. Synonymous changes do not alter amino acid sequence and therefore should not be damaging to the cell.

alogue between stem cell and cancer biologists will be needed as the rapid advances in genomic sequencing yield greater insights into the genesis of cancer. Further work is also needed to determine whether there is a consistently different mutational load in different starting somatic cell types influencing the choice of cellular source for iPS cell generation, and whether the mutational load increases dramatically with aging, which might justify the banking of neonatal cells. With the advent of high-density arrays and modern sequencing methods, even minor changes in genome integrity can be detected, allowing an extensive evaluation of genome integrity and mutational load. The mutational burden observed in iPS cells and its impact on clinical utility are critical issues that must be addressed before the broad therapeutic application of gene-corrected iPS cells in transplantation medicine.

Materials and Methods

iPS Cell Derivation and Culture. Patient fibroblasts were obtained from Coriell Laboratories (ID no. GM06330) and cultured in DMEM (Invitrogen) supplemented with 10% FBS (HyClone) at 37 °C, 5% CO_2, 5% O_2. The episomal plasmids and protocols used for reprogramming were described (12). After isolation, iPS cells were maintained and expanded in TeSR and passaged routinely with EDTA as described (23).

Transfection. Gene targeting experiments were performed by using conditions optimized for human ES cells (24). Cells were harvested with TrpLE (Invitrogen) and resuspended at a concentration of 5×10^6 cells per mL; 0.5 mL of the cell suspension was mixed with ≈50 μg of linearized gene targeting vector in 300 μL of PBS and electroporated in a 0.4-cm cuvettete. Cells were then plated on a 10-cm matrigel-coated dish in TeSR medium with 10 μM HA100 (Sigma). Puromycin was added to the culture medium (1 ng/mL) after 3 d. To remove the loxP-flanked selection, cassette cells were harvested and electroporated as described with 15 μg in vitro transcribed mRNA-encoding Cre recombinase.

FISH. Metaphase spreads were prepared according to a standard procedure. The *OAT* gene targeting vector, labeled with Spectrum Green-dUTP (Vysis), was used as the probe.

Genomic PCR and RT-PCR. Total genomic DNA was extracted by using the Nucleon BACC3 kit (GE Healthcare). Total RNA was extracted by using the RNeasy Plus Mini Kit (Qiagen). cDNA was synthesized by using SuperScript III (Invitrogen), according to the manufacturer's protocol. PCR was performed by using the Taq PCR Core Kit (Qiagen).

aCGH. A custom array was designed that consisted of the NimbleGen human CGH 2.1M Whole-Genome-Tiling v2.0D array in addition to 4,633 custom designed probes that cover the gene targeting construct and the reprogramming plasmid vectors used in this study. The original whole-genome-tilling design has the resolution of 5 kb over the entire human genome, whereas our custom fine-tilling design could detect 200-bp CNV regions. CGH experiments were performed at Roche NimbleGen and the WiCell Cytogenetics Laboratory (WiCell Research Institute). Experiments performed at WiCell involved a multistep labeling procedure as described (25). Data were analyzed using SignalMap software (Roche NimbleGen). aCHG data can be found at http://www.ncbi.nlm.nih.gov/geo/ under accession no. GSE26773.

Whole-Genome Library Construction. Whole-genome libraries for each cell line were constructed as described (4). Briefly, genomic DNA for each of the four samples was sheared by using a Covaris AFA and enzymatically end-repaired. Sheared DNA was then enzymatically ligated to common sequencing primers and amplified by using PCR to generate a whole-genome library.

In-Solution Hybridization Capture with DNA Baits. Whole-genome libraries were enriched for exomic regions by using the NimbleGen SeqCap EZ Exome kit. Libraries were denatured and hybridized to the SeqCap EZ Exome library and then captured using streptavidin beads by following the manufacturer's protocol. Enriched libraries were sequenced on an Illumina Genome Analyzer IIx.

Consensus Sequence Generation and Variant Calling. Novel reprogramming-associated mutations were identified as described (26). Briefly, Illumina GA IIx reads were filtered by using GERALD and mapped to the genome using Bowtie or BWA. Consensus sequence generation was performed by using SAMtools or GATK. Each iPS consensus sequence was directly compared with its progenitor consensus sequence, and candidate sites indicating a gain of a new allele in the iPS line were chosen.

Sanger Validation of Candidate Mutations. Each candidate mutation was validated via amplification with specially designed primers and capillary Sanger sequencing performed by GeneWiz.

ACKNOWLEDGMENTS. We thank Dr. David Frisch and Dr. Fred Blattner for providing the hES-2A–inducible BAC vector. This study is funded by a Wynn-Gund Translational Award from the Foundation Fighting Blindness and partially funded by the Charlotte Geyer Foundation and National Institutes of Health Grant R01 HL094963. S.E.H. is supported by a National Health and Medical Research Council Overseas Biomedical Fellowship. A.G. is supported by the Focht-Powell Fellowship and a California Institute for Regenerative Medicine predoctoral Fellowship.

1. Takahashi K, et al. (2007) Induction of pluripotent stem cells from adult human fibroblasts by defined factors. *Cell* 131:861–872.
2. Takahashi K, Yamanaka S (2006) Induction of pluripotent stem cells from mouse embryonic and adult fibroblast cultures by defined factors. *Cell* 126:663–676.
3. Yu J, et al. (2007) Induced pluripotent stem cell lines derived from human somatic cells. *Science* 318:1917–1920.
4. Gore A, et al. (2011) Somatic coding mutations in human induced pluripotent stem cells. *Nature* 471:63–67.

5. Simell O, Takki K (1973) Raised plasma-ornithine and gyrate atrophy of the choroid and retina. *Lancet* 1:1031–1033.
6. Wang T, Milam AH, Steel G, Valle D (1996) A mouse model of gyrate atrophy of the choroid and retina. Early retinal pigment epithelium damage and progressive retinal degeneration. *J Clin Invest* 97:2753–2762.
7. Gehrs KM, Anderson DH, Johnson LV, Hageman GS (2006) Age-related macular degeneration—emerging pathogenetic and therapeutic concepts. *Ann Med* 38: 450–471.
8. Buchholz DE, et al. (2009) Derivation of functional retinal pigmented epithelium from induced pluripotent stem cells. *Stem Cells* 27:2427–2434.
9. Meyer JS, et al. (2009) Modeling early retinal development with human embryonic and induced pluripotent stem cells. *Proc Natl Acad Sci USA* 106:16698–16703.
10. Carr AJ, et al. (2009) Protective effects of human iPS-derived retinal pigment epithelium cell transplantation in the retinal dystrophic rat. *PLoS ONE* 4:e8152.
11. Anonymous (2011) Stem-cell trial. *Nature* 469:137.
12. Yu J, et al. (2009) Human induced pluripotent stem cells free of vector and transgene sequences. *Science* 324:797–801.
13. Kirchmaier AL, Sugden B (1995) Plasmid maintenance of derivatives of oriP of Epstein-Barr virus. *J Virol* 69:1280–1283.
14. Sugden B, Warren N (1988) Plasmid origin of replication of Epstein-Barr virus, oriP, does not limit replication in cis. *Mol Biol Med* 5:85–94.
15. Laurent LC, et al. (2011) Dynamic changes in the copy number of pluripotency and cell proliferation genes in human ESCs and iPSCs during reprogramming and time in culture. *Cell Stem Cell* 8:106–118.
16. Mayshar Y, et al. (2010) Identification and classification of chromosomal aberrations in human induced pluripotent stem cells. *Cell Stem Cell* 7:521–531.
17. Lynch M (2010) Rate, molecular spectrum, and consequences of human mutation. *Proc Natl Acad Sci USA* 107:961–968.
18. Song H, Chung SK, Xu Y (2010) Modeling disease in human ESCs using an efficient BAC-based homologous recombination system. *Cell Stem Cell* 6:80–89.
19. Fraser MJ, Ciszczon T, Elick T, Bauser C (1996) Precise excision of TTAA-specific lepidopteran transposons piggyBac (IFP2) and tagalong (TFP3) from the baculovirus genome in cell lines from two species of Lepidoptera. *Insect Mol Biol* 5:141–151.
20. Woltjen K, et al. (2009) piggyBac transposition reprograms fibroblasts to induced pluripotent stem cells. *Nature* 458:766–770.
21. Zhou H, et al. (2009) Generation of induced pluripotent stem cells using recombinant proteins. *Cell Stem Cell* 4:381–384.
22. Warren L, et al. (2010) Highly efficient reprogramming to pluripotency and directed differentiation of human cells with synthetic modified mRNA. *Cell Stem Cell* 7:618–630.
23. Chen G, Hou Z, Gulbranson DR, Thomson JA (2010) Actin-myosin contractility is responsible for the reduced viability of dissociated human embryonic stem cells. *Cell Stem Cell* 7:240–248.
24. Zwaka TP, Thomson JA (2003) Homologous recombination in human embryonic stem cells. *Nat Biotechnol* 21:319–321.
25. Taapken SM, Nisler BS, Sampsell-Barron TL, Dyer Montgomery K (2010) Automation in an array comparative genomic hybridization laboratory improves throughput and data quality. *JALA* 15:390–395.
26. Quail MA, Swerdlow H, Turner DJ (2009) Improved protocols for the illumina genome analyzer sequencing system. *Curr Protoc Hum Genet* 62:18.2.1–18.2.27.